

## Forward Jet Production at the Large Hadron Collider

M. Deak,<sup>1</sup> F. Hautmann,<sup>2</sup> H. Jung,<sup>1</sup> and K. Kutak<sup>1</sup>

<sup>1</sup>*Deutsches Elektronen Synchrotron, D-22603 Hamburg*

<sup>2</sup>*Theoretical Physics, University of Oxford, Oxford OX1 3NP*

### Abstract

At the Large Hadron Collider (LHC) it will become possible for the first time to investigate experimentally the forward region in hadron-hadron collisions via high- $p_T$  processes. In the LHC forward kinematics QCD logarithmic corrections in the hard transverse momentum and in the large rapidity interval may both be quantitatively significant. We analyze the hadroproduction of forward jets in the framework of QCD high-energy factorization, which allows one to resum consistently both kinds of corrections to higher orders in QCD perturbation theory. We compute the short-distance matrix elements needed to evaluate the factorization formula at fully exclusive level. We discuss numerically dynamical features of multi-gluon emission at large angle encoded in the factorizing high-energy amplitudes.

## I. INTRODUCTION

Experiments at the Large Hadron Collider (LHC) will explore the region of large rapidities both with general-purpose detectors and with dedicated instrumentation, including forward calorimeters and proton taggers [1, 2, 3, 4, 5, 6, 7]. The forward-physics program involves a wide range of topics, from new particle discovery processes [3, 8, 9] to new aspects of strong interaction physics [7, 10, 11] to heavy-ion collisions [12, 13]. Owing to the large center-of-mass energy and the unprecedented experimental coverage at large rapidities, it becomes possible for the first time to investigate the forward region with high- $p_T$  probes.

The hadroproduction of a forward jet associated with a hard final state  $X$  is pictured in Fig. 1. The kinematics of the process is characterized by the large ratio of sub-energies  $s_1/s \gg 1$  and highly asymmetric longitudinal momenta in the partonic initial state,  $k_1 \cdot p_2 \gg k_2 \cdot p_1$ . At the LHC the use of forward calorimeters allows one to measure events where jet transverse momenta  $p_T > 20$  GeV are produced several units of rapidity apart,  $\Delta y \gtrsim 4 \div 6$  [1, 5, 7]. Working at polar angles that are small but sufficiently far from the beam axis not to be affected by beam remnants, one measures azimuthal plane correlations between high- $p_T$  events widely separated in rapidity (Fig. 2).

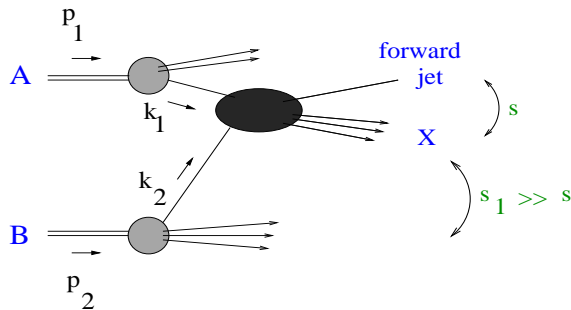


FIG. 1: Jet production in the forward rapidity region in hadron-hadron collisions.

The presence of multiple large-momentum scales implies that, as was recognized in [14, 15, 16], reliable theoretical predictions for forward jets can only be obtained after summing logarithmic QCD corrections at high energy to all orders in  $\alpha_s$ . This has motivated efforts [17, 18, 19, 20] to construct new algorithms for Monte Carlo event generators capable of describing jet production beyond the central rapidity region. Note that an analogous observation applies to forward jets associated to deeply inelastic scattering [21, 22]. Indeed, measurements of forward jet cross sections at HERA [23] indicate that neither fixed-order next-to-leading calculations nor standard shower Monte Carlo generators [17, 23, 24], e.g. PYTHIA or HERWIG, are able to describe forward jet  $ep$  data. Improved methods to evaluate QCD predictions are needed to treat the multi-scale region implied by the forward kinematics.

In this work we move on from the observation that realistic phenomenology in the LHC forward region will require taking into account at higher order both logarithmic corrections in the large rapidity interval (of high-energy type) and logarithmic corrections in the hard transverse momentum (of collinear type). The theoretical framework to resum consistently both kinds of logarithmic corrections in QCD perturbation theory is based on high-energy factorization at fixed transverse momentum [25].

This formulation depends on unintegrated distributions for parton splitting, obeying ap-



FIG. 2: (Left) High- $p_T$  events in the forward and central detectors; (right) azimuthal plane segmentation.

appropriate evolution equations, and short-distance, process-dependent matrix elements. The unintegrated-level evolution is given by evolution equations in rapidity, or angle, parameters. Different forms of the evolution, valid in different kinematic regions, are available. See [26, 27, 28, 29], and references therein, for recent work in this area and reviews. The short-distance matrix elements, needed in the evaluation of the factorization formula, are the subject of this paper. We obtain their explicit expressions in a fully exclusive form, including all partonic channels, and present results of numerically integrating them over final states. Such matrix elements, though not on shell, are gauge invariant and perturbatively calculable. They factorize in the high energy limit in front of (unintegrated) distributions for parton splitting not only in the collinear emission region but also at finite angle. In particular, they can serve to take into account effects of coherence from multi-gluon emission, away from small angles, which become important for correlations among jets across long separations in rapidity. We give a numerical illustration of the high- $k_T$  behavior resulting from such finite-angle radiation.

On one hand, once convoluted with the small- $x$  gluon Green's function according to the method [25, 30], these matrix elements control the summation of high-energy logarithmic corrections, contributing both to the next-to-leading-order BFKL kernel [31] and to the jet impact factors [32, 33]. On the other hand, they can be used in a shower Monte Carlo implementing parton-branching kernels at unintegrated level (see e.g. [34, 35] for recent works) to generate fully exclusive events. We leave these applications to a separate paper.

The paper is organized as follows. After recalling the factorized form of the cross sections in Sec. II, we present the high-energy amplitudes in Sec. III, and discuss basic properties and numerical results in Sec. IV. We summarize in Sec. V.

## II. HIGH-ENERGY FACTORIZED CROSS SECTIONS

High-energy factorization [25] allows one to decompose the cross section for the process of Fig. 1 into partonic distributions (in general, unintegrated) and hard-scattering kernels, obtained via the high-energy projectors [25, 30] from the amplitudes for the process  $p_1 + p_2 \rightarrow p_3 + p_4 + 2$  massless partons. The basic structure is depicted in Fig. 3.

With reference to the notation of Fig. 3, let us work in the center of mass frame of the incoming momenta

$$p_1 = \sqrt{S/2}(1, 0, 0_T) \quad , \quad p_2 = \sqrt{S/2}(0, 1, 0_T) \quad , \quad 2p_1 \cdot p_2 = S \quad , \quad (1)$$

where, for any four-vector,  $p^\mu = (p^+, p^-, p_T)$ , with  $p^\pm = (p^0 \pm p^3)/\sqrt{2}$  and  $p_T$  two-dimensional euclidean vector. Let us parameterize the exchanged momenta in terms of purely transverse four-vectors  $k_\perp$  and  $k_{\perp 1}$  and longitudinal momentum fractions  $\xi_i$  and  $\bar{\xi}_i$  as

$$p_1 - p_5 = k_1 = \xi_1 p_1 + k_{\perp 1} + \bar{\xi}_1 p_2 \quad , \quad p_2 - p_6 = k_2 = \xi_2 p_2 + k_\perp + \bar{\xi}_2 p_1 \quad . \quad (2)$$

For high energies we can introduce strong ordering in the longitudinal momenta,  $\xi_1 \gg |\bar{\xi}_2|$ ,  $\xi_2 \gg |\bar{\xi}_1|$ . Further, we make the forward region approximations  $(p_4 + p_6)^2 \gg (p_3 + p_4)^2$ ,  $k_1 \simeq \xi_1 p_1$ ,  $k_2 \simeq \xi_2 p_2 + k_\perp$ , so that

$$p_5 \simeq (1 - \xi_1)p_1 \quad , \quad p_6 \simeq (1 - \xi_2)p_2 - k_\perp \quad , \quad \xi_1 \gg \xi_2 \quad . \quad (3)$$

It is convenient to define the rapidity-weighted average of dijet transverse momenta,

$$Q_T = (1 - \nu)p_{T4} - \nu p_{T3} \quad , \quad \text{where} \quad \nu = (p_2 p_4) / [(p_2 p_1) - (p_2 p_5)] \quad , \quad (4)$$

and the azimuthal angle

$$\cos \varphi = Q_T \cdot k_T / |Q_T| |k_T| \quad . \quad (5)$$

We consider the differential jet cross section in  $Q_T$  and  $\varphi$ .



FIG. 3: (a) Factorized structure of the cross section; (b) a graph contributing to the  $qg$  channel matrix element.

According to the factorization [25, 32], the jet cross section can be computed as (Fig. 3a)

$$\frac{d\sigma}{dQ_T^2 d\varphi} = \sum_a \int d\xi_1 d\xi_2 d^2 k_T \phi_{a/A}(\xi_1) \frac{d\hat{\sigma}}{dQ_T^2 d\varphi}(\xi_1 \xi_2 S, k_T, Q_T, \varphi) \phi_{g^*/B}(\xi_2, k_T) \quad , \quad (6)$$

where the sum goes over parton species,  $\phi$  are the parton distributions defined from the unintegrated Green's functions introduced in [30] for both gluon and quark cases, and  $\hat{\sigma}$  is the hard cross section, calculable from the high-energy limit of perturbative amplitudes (Fig. 3b).

The physical picture underlying Eq. (6) is based on the fact that initial-state parton configurations contributing to forward production are asymmetric, with the parton in the top subgraph being probed near the mass shell and large  $x$ , while the parton in the bottom subgraph is off-shell and small- $x$ . Eq. (6) embodies this picture through the longitudinal and transverse momentum dependences of both  $\phi$  and  $\hat{\sigma}$ .

For phenomenological studies we will be interested in coupling Eq. (6) to parton showers to achieve a full description of the associated final states. To this end we need the matrix elements defining the hard-scattering kernels in a fully exclusive form. We give the results in the next section.

### III. MATRIX ELEMENTS FOR FULLY EXCLUSIVE EVENTS

The matrix elements determining the hard-scattering kernels  $\hat{\sigma}$  can be viewed as a suitably defined off-shell continuation of scattering amplitudes at lower order [25]. They can be obtained by applying to scattering amplitudes  $\mathcal{M}$  the high-energy eikonal projectors [25, 30],

$$\mathcal{M}^H = P_{(eik)}^H{}^{\mu_1\mu_2\dots} \mathcal{M}_{\mu_1\mu_2\dots}(k_1, k_2, \{p_i\}) \quad , \quad P_{(eik)}^H{}^{\mu_1\mu_2\dots} \propto \frac{2k_{\perp 1}^{\mu_1} k_{\perp 2}^{\mu_2}}{\sqrt{k_{\perp 1}^2 k_{\perp 2}^2}} \quad . \quad (7)$$

Although they are not evaluated on shell, they are gauge invariant and their expressions are simple. The utility of these matrix elements is that in the high-energy limit they factorize not only in the collinear emission region but also in the large-angle emission region. As long as the factorization is carried out in terms of distributions for parton splitting at fixed transverse momentum, as in Eq. (6), they can be useful to include coherence effects [32] from multi-gluon emission across large rapidity intervals, not associated with small angles.

The results for the matrix elements in exclusive form are given by

$$\mathcal{M}_{qg \rightarrow qg} = C_1 \mathcal{A}_1^{(ab)} + \bar{C}_1 \mathcal{A}_1^{(nab)} \quad , \quad \mathcal{M}_{gg \rightarrow q\bar{q}} = C_2 \mathcal{A}_2^{(ab)} + \bar{C}_2 \mathcal{A}_2^{(nab)} \quad , \quad \mathcal{M}_{gg \rightarrow gg} = C_3 \mathcal{A}_3 \quad (8)$$

where

$$\mathcal{A}_1^{(ab)} = \left( \frac{k_1 k_2}{k_1 p_2} \right)^2 \frac{(k_1 p_2)^2 + (p_2 p_3)^2}{(k_1 p_4) (p_3 p_4)} \quad , \quad (9)$$

$$\mathcal{A}_1^{(nab)} = \left( \frac{k_1 k_2}{k_1 p_2} \right)^2 \frac{(k_1 p_2)^2 + (p_2 p_3)^2}{(k_1 p_4) (p_3 p_4)} \left( \frac{(p_3 p_4) (k_1 p_2)}{(k_1 p_3) (p_2 p_4)} + \frac{(k_1 p_4) (p_2 p_3)}{(k_1 p_3) (p_2 p_4)} - 1 \right) \quad , \quad (10)$$

$$\mathcal{A}_2^{(ab)} = \left( \frac{k_1 k_2}{k_1 p_2} \right)^2 \frac{(p_2 p_3)^2 + (p_2 p_4)^2}{(k_1 p_4) (k_1 p_3)} \quad , \quad (11)$$

$$\mathcal{A}_2^{(nab)} = \left( \frac{k_1 k_2}{k_1 p_2} \right)^2 \frac{(p_2 p_3)^2 + (p_2 p_4)^2}{(k_1 p_4) (k_1 p_3)} \left( \frac{(k_1 p_4) (p_2 p_3)}{(p_3 p_4) (k_1 p_2)} + \frac{(k_1 p_3) (p_2 p_4)}{(p_3 p_4) (k_1 p_2)} - 1 \right) \quad , \quad (12)$$

$$\mathcal{A}_3 = \left( \frac{k_1 k_2}{k_1 p_2} \right)^2 \frac{(p_3 p_4)(k_1 p_2) + (k_1 p_4)(p_2 p_3) + (p_2 p_4)(k_1 p_3)}{(p_2 p_4)(k_1 p_4)(p_3 p_4)(k_1 p_2)(p_2 p_3)(k_1 p_3)} \left[ (p_2 p_4)^4 + (k_1 p_2)^4 + (p_2 p_3)^4 \right] \quad , \quad (13)$$

and  $C_1 = g^4(N_c^2 - 1)/(4N_c^2)$ ,  $\bar{C}_1 = C_1 C_A/(2C_F)$ ,  $C_2 = g^4/(2N_c)$ ,  $\bar{C}_2 = C_2 C_A/(2C_F)$ ,  $C_3 = g^4 N_c^2/(N_c^2 - 1)$ .

The results above contain the dependence on the transverse momentum  $k_{\perp}$  along the parton lines that connect the hard scatter to the parton distributions. Nevertheless, they are short-distance in the sense that they can be safely integrated down to  $k_{\perp} = 0$ . That is, the high-energy projection is designed so that all infrared contributions are factored out in the nonperturbative Green's functions  $\phi$  in Eq. (6). An explicit numerical illustration is given in the next section.<sup>1</sup>

---

<sup>1</sup> Although the hard-scattering functions constructed from the amplitudes in Eqs. (9)-(13) are not coefficient functions in the conventional sense of the operator product expansion, they can be related to such objects, for inclusive variables, along the lines e.g. of [30]. They could be interpreted in terms of coefficient functions in the sense of the high-energy OPE of [36].

The role of Eqs. (9)-(13) is twofold. On one hand, they give the high-energy limit of multi-parton matrix elements in the forward region, which may be of direct phenomenological significance. On the other hand, because of the factorization theorem [25], logarithmically enhanced corrections for large rapidity can be systematically obtained to all orders in  $\alpha_s$  from those in the (unintegrated) distributions for parton splitting once the hard scattering functions are known at finite  $k_\perp$ . To this end the detailed form of the fall-off at large  $|k_\perp|^2$  is relevant.

In the next section we discuss the behavior at high transverse momentum numerically. This behavior reflects properties of gluon emission at large angle encoded in the high-energy amplitudes. These are relevant, along with large-angle effects in the Sudakov region (see e.g. [37]), to achieve a full treatment of gluon coherence effects [38] capable of describing jet final states across the whole rapidity phase space. A uniform treatment of the high-energy and Sudakov regions is still an open issue [39] of interest for parton-shower implementations.

#### IV. NUMERICAL RESULTS

We now partially integrate the amplitudes over final states. We work at the level of hard scattering matrix elements, leaving the treatment of parton evolution by showering to a separate study [40]. We concentrate on the region of hard emissions, where jets are well separated. Regions near the boundary of the angular phase space are sensitive to infrared radiation and can be addressed within a full parton-shower description of the process.

We consider the differential distribution in the transverse variable  $Q_T$  and azimuthal angle  $\varphi$ . The variable  $Q_T$  describes the imbalance in transverse momentum between the hardest jets, weighted by  $\nu$ , according to Eq. (4). In Figs. 4 and 5 we show numerical results versus transverse momentum and versus energy ( $qg$  channel).

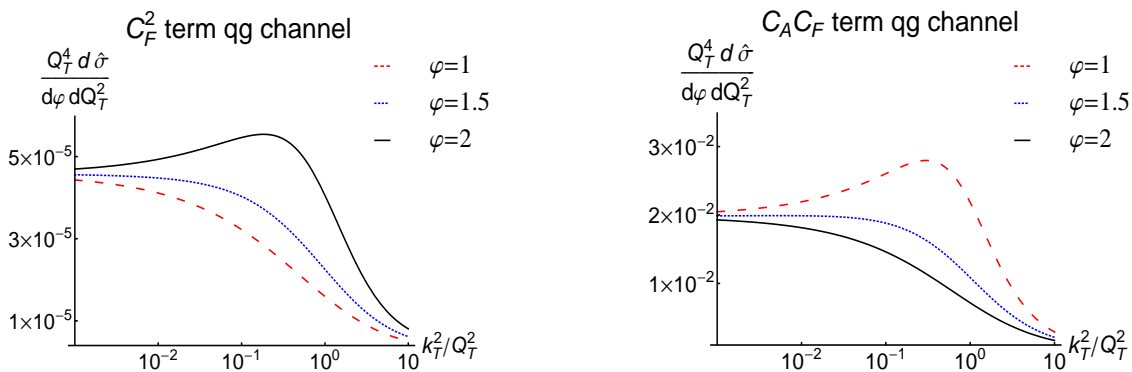


FIG. 4: The  $k_T/Q_T$  dependence of the factorizing  $qg$  hard cross section at high energy: (left)  $C_F^2$  term; (right)  $C_F C_A$  term ( $\xi_1 \xi_2 S/Q_T^2 = 10^2$ ,  $\alpha_s = 0.2$ ).

The curves in Fig. 4 measure the  $k_T$  distribution of the jet system recoiling against the leading di-jets. The result at  $k_T/Q_T \rightarrow 0$  in these plots returns the lowest-order result, i.e., the leading-order process with two back-to-back jets,

$$\frac{d\hat{\sigma}}{dQ_T^2 d\varphi} \rightarrow \alpha_s^2 f^{(0)}(p_T^2/s) \quad , \quad Q_T \rightarrow p_T = |p_{T3}| = |p_{T4}| \quad , \quad (14)$$

where  $s = (p_3 + p_4)^2$ , and  $f^{(0)}$  is given by

$$f^{(0)}(z) = \frac{1}{16\sqrt{1-4z}} [C_F^2 z(1+z) + 2C_F C_A(1-3z+z^2)] . \quad (15)$$

The dependence on  $k_T$  and  $\varphi$  plotted in Fig. 4 is the result of higher-order gluon radiation, treated according to the high-energy asymptotics. The different behaviors in  $\varphi$  for the  $C_F^2$  and  $C_A C_F$  terms reflect the fact that the former comes from the insertion of gluons on fermion-exchange amplitude while the latter comes from the insertion of gluons on vector-exchange amplitude.

Fig. 5 shows the energy dependence for fixed  $k_T/Q_T$ . The constant asymptotic behavior at large  $s$  due to color-octet spin-1 exchange distinguishes the  $C_F C_A$  term from the  $C_F^2$  term. The dependence on the azimuthal angle in Figs. 4 and 5 is relevant, especially because forward jet measurements will rely on azimuthal plane correlations between jets far apart in rapidity (Fig.2).

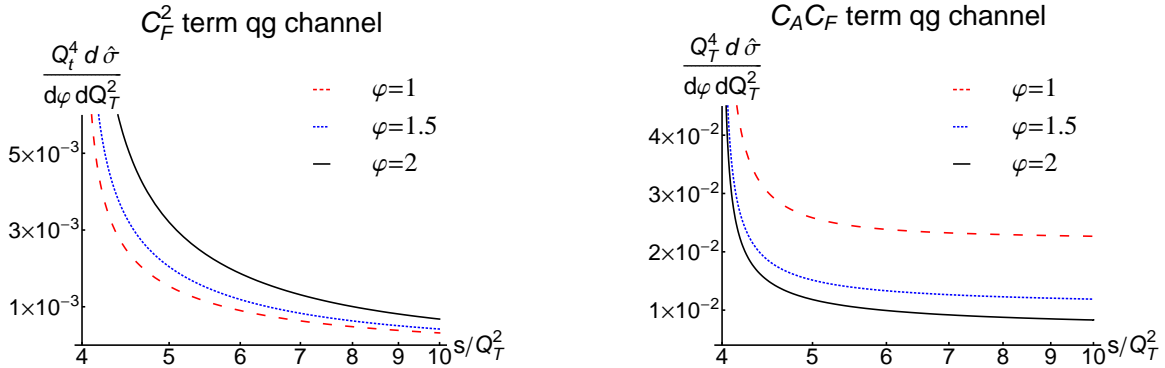


FIG. 5: The energy dependence of the  $qq$  hard cross section ( $k_T/Q_T = 1$ ).

While Eq. (15) gives the collinear emission limit, we see from Fig. 4 that multi-gluon radiation at finite angles sets a dynamical cut-off at values of  $k_T$  of order  $Q_T$ ,

$$k_T \lesssim \mu = c Q_T . \quad (16)$$

The physical meaning of this result is that the summation of the higher-order logarithmic corrections for large  $y \sim \ln s/p_T^2$  is precisely determined [25, 32] by convoluting the unintegrated splitting functions over the  $k_T$ -dependence in Fig. 4, via the distributional relation

$$\int d^2 k_T \left( \frac{1}{k_T^2} \right)_+ \hat{\sigma}(k_T) = \int d^2 k_T \frac{1}{k_T^2} [\hat{\sigma}(k_T) - \Theta(\mu - k_T) \hat{\sigma}(0_T)] . \quad (17)$$

So the results in Fig. 4 illustrate quantitatively the significance of contributions with  $k_T \simeq Q_T$  in the large- $y$  region. Non-negligible effects arise at high energy from the finite- $k_T$  tail. These effects are not included in collinear-branching generators (and only partially in fixed-order perturbative calculations), and become more and more important as the jets are observed at large rapidity separations.

Observe that calculations based on the unintegrated formalism will in general depend on two scales,  $\mu$  and the rapidity, or angle, cut-off [26, 39, 41]. See e.g. the one-loop

calculation [29] for an explicit example. It will be of interest to investigate the effect of Eq. (16) on the behavior in rapidity distributions [40].

Results for gluon-gluon channels are reported in Fig. 6. Note the large effect of the purely gluonic component. The behavior versus  $k_T$  is qualitatively similar to that in Fig. 4. Calculations in progress [40], including parton showering, indicate that quark and gluon channels give contributions of comparable size in the LHC forward kinematics. The inclusion of both is relevant for realistic studies of phenomenology [11, 42]. Since the forward kinematics selects asymmetric parton momentum fractions, effects due to the  $x \rightarrow 1$  endpoint behavior [29, 43] at fixed transverse momentum may become phenomenologically significant as well.

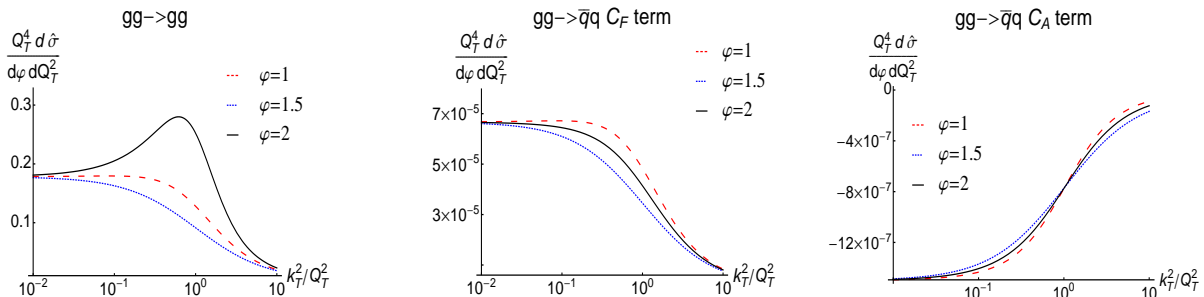


FIG. 6: The  $k_T/Q_T$  dependence of the factorizing  $gg$  matrix elements: (a)  $gg \rightarrow gg$ ; (b)  $gg \rightarrow q\bar{q}$   $C_F$  term; (c)  $gg \rightarrow q\bar{q}$   $C_A$  term ( $\xi_1 \xi_2 S/Q_T^2 = 10^2$ ,  $\alpha_s = 0.2$ ).

We conclude this section by recalling that dynamical effects of high parton densities have been studied [10, 44] as potential contributions to forward jet events. We note that if such effects show up at the LHC, the unintegrated formulation discussed above would likely be the natural framework to implement this dynamics at parton-shower level.

## V. CONCLUSIONS

Forward + central detectors at the LHC allow jet correlations to be measured across rapidity intervals of several units,  $\Delta y \gtrsim 4 \div 6$ . Such multi-jet states can be relevant to new particle discovery processes as well as new aspects of standard model physics.

Existing sets of forward-jet data in ep collisions, much more limited than the potential LHC yield, indicate that neither conventional parton-showering Monte Carlo generators nor next-to-leading-order QCD calculations are capable of describing forward jet phenomenology. These observations motivate studies of improved methods to compute QCD predictions in the multiple-scale kinematics implied by the forward region.

We have analyzed the high-energy factorization that serves to sum consistently to higher orders in  $\alpha_s$  both the logarithmic corrections in the large rapidity interval and those in the hard jet transverse energy. We have determined the gauge-invariant (though not on shell) high-energy amplitudes, which are needed to evaluate the factorization formula for forward jet hadroproduction.

Our results can be used along with  $k_\perp$ -dependent kernels for parton branching. They can serve to construct predictions for exclusive observables associated to forward jets, including



jet correlations, that take into account gluon coherence not only in the collinear emission region but also in the large-angle emission region.

**Acknowledgments.** One of us (F.H.) visited DESY at various stages while this work was being done and wishes to thank the DESY directorate for hospitality and support. Part of this work was carried out during the 2009 DESY Institute on Parton Showers and Resummations. We thank the organizers and participants in the workshop for the stimulating atmosphere. We gratefully acknowledge useful discussions with S. Baranov, J. Collins, A. Knutsson, A. Lipatov, Z. Nagy, T. Rogers and N. Zotov.

- 
- [1] CMS Coll., CERN-LHCC-2006-001 (2006); CMS PAS FWD-08-001 (2008).
  - [2] ATLAS Coll., CERN-LHCC-2008-004 (2008); CERN-LHCC-2007-001 (2007).
  - [3] M.G. Albrow et al., FP420 Coll., arXiv:0806.0302 [hep-ex].
  - [4] CMS Coll., TOTEM Coll., CERN-LHCC-2006-039/G -124 (2006).
  - [5] X. Aslanoglou et al., CERN-CMS-NOTE-2008-022 (2008); Eur. Phys. J. C **52** (2008) 495.
  - [6] M. Grothe, arXiv:0901.0998 [hep-ex].
  - [7] H. Jung et al., Proc. Workshop “HERA and the LHC”, arXiv:0903.3861 [hep-ph].
  - [8] A. De Roeck et al., Eur. Phys. J. C **25** (2002) 391.
  - [9] S. Heinemeyer et al., Eur. Phys. J. C **53** (2008) 231.
  - [10] D. d’Enterria, arXiv:0806.0883 [hep-ex]; Eur. Phys. J. A **31** (2007) 816.
  - [11] S. Cerci and D. d’Enterria, arXiv:0812.2665 [hep-ex], AIP Conf. Proc. 1105 (2009) 28.
  - [12] A. Accardi et al., CERN-2004-009-B, CERN-2004-009-A; hep-ph/0308248.
  - [13] CMS Coll., CERN-LHCC-2007-009 (2007).
  - [14] A.H. Mueller and H. Navelet, Nucl. Phys. **B282** (1987) 727.
  - [15] V. Del Duca, M.E. Peskin and W.K. Tang, Phys. Lett. **B306** (1993) 151.
  - [16] W.J. Stirling, Nucl. Phys. **B423** (1994) 56.
  - [17] C. Ewerz, L.H. Orr, W.J. Stirling and B.R. Webber, J. Phys. **G26** (2000) 696; J. Forshaw, A. Sabio Vera and B.R. Webber, J. Phys. **G25** (1999) 1511.
  - [18] L.H. Orr and W.J. Stirling, Phys. Lett. **B436** (1998) 372.
  - [19] J.R. Andersen, V. Del Duca, S. Frixione, F. Maltoni, C.R. Schmidt and W.J. Stirling, hep-ph/0109019; J.R. Andersen, V. Del Duca, S. Frixione, C.R. Schmidt and W.J. Stirling, JHEP **0102** (2001) 007.
  - [20] J.R. Andersen, arXiv:0906.1965 [hep-ph]; J.R. Andersen and C.D. White, Phys. Rev. **D78** (2008) 051501, J.R. Andersen and A. Sabio Vera, Phys. Lett. **B567** (2003) 116.
  - [21] A.H. Mueller, Nucl. Phys. B Proc. Suppl. **18C** (1990) 125.
  - [22] W.K. Tang, Phys. Lett. **B278** (1992) 363; J. Bartels, A. De Roeck and M. Loewe, Z. Phys. **C54** (1992) 635; J. Kwiecinski, A.D. Martin and P.J. Sutton, Phys. Rev. **D46** (1992) 921; S. Catani, M. Ciafaloni and F. Hautmann, Nucl. Phys. B Proc. Suppl. **29A** (1992) 182.
  - [23] A. Aktas et al., Eur. Phys. J. **C46** (2006) 27; S. Chekanov et al., Phys. Lett. **B632** (2006) 13.
  - [24] B.R. Webber, hep-ph/9510283, in Proc. Workshop DIS95.
  - [25] S. Catani, M. Ciafaloni and F. Hautmann, Phys. Lett. **B307** (1993) 147; Nucl. Phys. **B366** (1991) 135; Phys. Lett. **B242** (1990) 97.
  - [26] J.C. Collins, arXiv:0808.2665 [hep-ph], PoS LC2008 (2008) 028.

- [27] F. Hautmann, Acta Phys. Polon. B **40** (2009) 2139.
- [28] T.C. Rogers, Phys. Rev. D **78** (2008) 074018.
- [29] F. Hautmann, Phys. Lett. B**655** (2007) 26.
- [30] S. Catani and F. Hautmann, Nucl. Phys. B**427** (1994) 475; Phys. Lett. B**315** (1993) 157.
- [31] V.S. Fadin and L.N. Lipatov, Phys. Lett. B**429** (1998) 127; G. Camici and M. Ciafaloni, Phys. Lett. B**430** (1998) 349.
- [32] M. Ciafaloni, Phys. Lett. B**429** (1998) 363.
- [33] F. Schwennsen, hep-ph/0703198; J. Bartels, A. Sabio Vera and F. Schwennsen, arXiv:0709.3249, JHEP **0611** (2006) 051; J. Bartels, D. Colferai and G.P. Vacca, Eur. Phys. J. C**29** (2003) 235; Eur. Phys. J. C**24** (2002) 83.
- [34] S. Jadach and M. Skrzypek, arXiv:0905.1399 [hep-ph].
- [35] F. Hautmann and H. Jung, JHEP **0810** (2008) 113; arXiv:0804.1746 [hep-ph].
- [36] I. Balitsky, Phys. Rev. D**72** (2005) 074027.
- [37] Yu.L. Dokshitzer and G. Marchesini, JHEP **0601** (2006) 007.
- [38] Yu.L. Dokshitzer, V.A. Khoze, A.H. Mueller and S.I. Troian, Rev. Mod. Phys. **60** (1988) 373; M. Ciafaloni, in *Perturbative Quantum Chromodynamics*, ed. A.H. Mueller (World Scientific, Singapore, 1989).
- [39] J.R. Andersen et al., Eur. Phys. J. C**48** (2006) 53.
- [40] M. Deak, F. Hautmann, H. Jung and K. Kutak, in preparation.
- [41] J.C. Collins, hep-ph/0106126, in Proc. Workshop DIS01.
- [42] A. Sabio Vera and F. Schwennsen, Nucl. Phys. B**776** (2007) 170; C. Marquet and C. Royon, Phys. Rev. D**79** (2009) 034028; P. Aurenche, R. Basu and M. Fontannaz, Eur. Phys. J. C **57** (2008) 681; M. Fontannaz, LPT-Orsay preprint (April 2009).
- [43] J.C. Collins and F. Hautmann, JHEP **0103** (2001) 016; Phys. Lett. B **472** (2000) 129.
- [44] E. Iancu, M.S. Kugeratski and D.N. Triantafyllopoulos, Nucl. Phys. A**808** (2008) 95; Y. Hatta, E. Iancu and A.H. Mueller, JHEP **0801** (2008) 026; E. Iancu, C. Marquet and G. Soyez, Nucl. Phys. A **780** (2006) 52; C. Marquet and R. B. Peschanski, Phys. Lett. B **587** (2004) 201.